FLATNESS-BASED TRAJECTORY TRACKING CONTROL OF A ROTATING SHAFT

Johannes v. Löwis, Joachim Rudolph
Institut für Regelungs- und Steuerungstheorie, Technische Universität Dresden, Germany
{loewis,rudolph}@erss11.et.tu-dresden.de
Jürgen Thiele, Frank Urban
AXOMAT GmbH, Berggießhübel, Saxony, Germany
axomat@t-online.de

ABSTRACT

Control of a magnetically levitated shaft used for drilling non-circular holes is considered. For this drilling process the shaft position must track a given reference trajectory determining the shape of the hole. The flatness property of the shaft model simplifies the design of a tracking controller. The system state as well as certain disturbances (due to model inaccuracies and drilling forces) are estimated by means of an observer. The usefulness of the proposed flatness-based trajectory tracking controller is demonstrated by experimental results obtained with a spindle built at the German company AXOMAT, Berggießhübel.

INTRODUCTION

One of the numerous advantages of using electromagnetic bearings for the support of a rotating shaft is that the shaft can be freely positionned on a prescribed path. However, the control of the shaft allowing one to exploit this feature is more involved than the stabilization at a desired position which is fixed in space. In this contribution we propose a flatness-based trajectory tracking controller for a shaft to be used for precision drilling of non-circular holes. In this application, the trajectories determine the shape of the hole.

The nonlinear nature of the process dynamics is important in the tracking application. This nonlinearity is due on the one hand to the rigid body dynamics and on the other hand to the relations between coil currents and forces. However, the nonlinear mathematical model is *differentially flat* [1, 3]. This means that the time evolution, i. e., the trajectories, of all system variables are completely determined by the trajectories of a finite set of variables, the so-called *flat output*, the trajectories of which can (in principle) be freely chosen (see also the appendix for the notion of flatness). On the basis of this mathematical property relatively simple controllers can be designed. These controllers are most appropriate for trajectory tracking. An additional feature of the nonlinear control law is the suppression of the steady state currents required with the classical linear control laws. This has been proposed by J. Lévine, J. Lottin, and J.-Ch. Ponsart [2, 4].

In this contribution the flatness-based control approach is discussed and results are presented that have been achieved with a rotating shaft designed at the German company AXOMAT in Berggießhübel, Saxony [8]. This device is equipped with five pairs of electromagnets which support a rotating shaft in its radial and the axial directions. The system, thus, has eleven inputs: the currents through the coils of the electromagnets and the torque produced by the motor. However, only one force is created by each pair of coils, and considering the resulting force as the input reduces the number of controls to six (the sixth one is the motor torque).

The paper is structured as follows: First we describe the drilling-process in some detail and highlight some of the problems to be tackled by the controller. We will also state the mathematical model of the system, which forms the basis for the controller design. The next section treats the design of the flatness-based trajectory tracking controller. The controller needs information about the system state as well as disturbances acting on the system. This information is obtained by an observer described in the following section. Finally, we present some results achieved with the proposed controller and some conclusions are drawn.

PROBLEM FORMULATION AND DESCRIPTION OF THE PROCESS

Control of a drilling-process is considered, where the hole to be drilled is non-circular — there is an industrial demand for tools that can be used for drilling such holes, for example by constructors of combustion engines. Specifically, the problem is: given a circular hole with a diameter of about 25mm, we want to give this

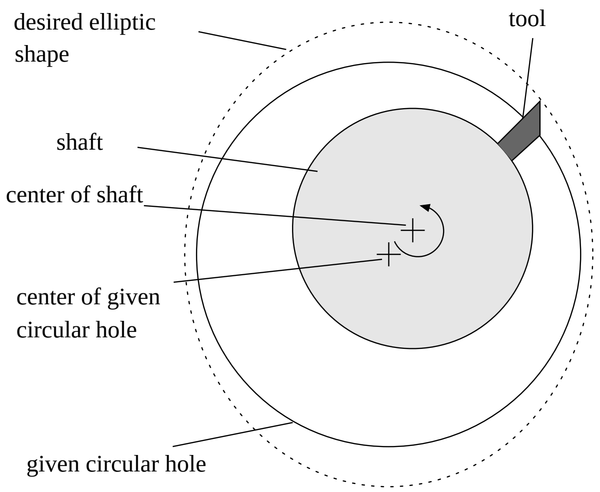

FIGURE 1: Sketch of the given circular hole and the desired elliptic hole

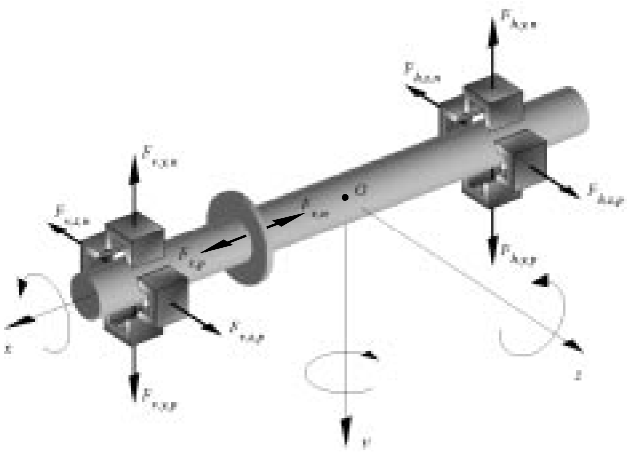

FIGURE 2: The shaft with its radial magnetic bearings

hole a slightly non-circular shape, for example an elliptic shape with major axis length 25.10mm and minor axis length 25.05mm. Figure 1 illustrates the situation.

For a circular hole the cutting edge of the tool has to be moved on a circular path. This already happens when the shaft rotates about an axis fixed in space. When drilling an elliptic hole the path of the cutting edge must be an ellipse. This can be achieved by moving the whole shaft on an elliptic path in such a way that this motion *is synchronized with the rotation* of the shaft. Thus, we have a trajectory tracking problem which is rather demanding, especially at high angular velocities of the shaft.

The setup is rather standard [7]. For further reference we state the model equations:

$$m\,\ddot{X} = \underbrace{F_{x,p} - F_{x,n}}_{F_x} + m\,g_x \tag{1a}$$

$$m\,\ddot{Y} = \underbrace{F_{v,y,p} - F_{v,y,n}}_{F_{v,y}} + \underbrace{F_{h,y,p} - F_{h,y,n}}_{F_{h,y}} + m\,g_y \tag{1b}$$

$$m\,\ddot{Z} = \underbrace{F_{v,z,p} - F_{v,z,n}}_{F_{v,z}} + \underbrace{F_{h,z,p} - F_{h,z,n}}_{F_{h,z}} + m\,g_z \tag{1c}$$

$$\Theta_2\,\ddot{\psi} = -(l_{f,v} - X)F_{v,z} + (l_{f,h} + X)F_{h,z} - \Theta_1\,\dot{\phi}\,\dot{\theta} \tag{1d}$$

$$\Theta_2\,\ddot{\theta} = \quad (l_{f,v} - X)F_{v,y} - (l_{f,h} + X)F_{h,y} + \Theta_1\,\dot{\phi}\,\dot{\psi} \tag{1e}$$

$$\Theta_1\,\ddot{\phi} = D_\phi. \tag{1f}$$

Here X, Y, and Z are the coordinates of the center of mass G of the shaft in a frame (with axes x, y, and z) fixed in space, at a point being considered as the "center" of the device. The angles ϕ, ψ, and θ describe the angular position of the axes of a body-fixed frame. The coil forces are denoted by $F_\bullet$, the motor torque as D_ϕ. (Here and in the sequel bullets ($\bullet$) are to be replaced by appropriate indices.) The shaft has mass m and moments of inertia Θ_1 and Θ_2; $l_{f,v}$ and $l_{f,h}$ are the distances between the planes of symmetry of the bearings (where the forces $F_\bullet$ are produced) and the point G. The forces are related with the currents by

$$F_\bullet = k_\bullet \frac{i_\bullet^2}{(\sigma_\bullet - s_\bullet)^2} \tag{2}$$

where the displacements from the magnetic centers are given by

$$\begin{aligned} s_{v,y,\bullet} &= \pm(Y + l_{f,v}\theta) \qquad & s_{h,y,\bullet} &= \pm(Y - l_{f,h}\theta) \\ s_{v,z,\bullet} &= \pm(Z - l_{f,v}\psi) \qquad & s_{h,z,\bullet} &= \pm(Z + l_{f,h}\psi) \\ s_{x,p} &= -s_{x,n} = X. \end{aligned} \tag{3}$$

The system has eleven inputs: the currents through the coils of the electromagnets and the torque produced by the motor (not shown in Figure 2). However, only one force is created by each pair of coils, and considering the resulting force as the input reduces the number of controls to six: F_x, $F_{v,y}$, $F_{h,y}$, $F_{v,z}$, $F_{h,z}$, D_ϕ. In the controller the ten coil currents can be computed from the five forces. This can be done in such a way that at each time instant only the current creating a force in the direction of the resulting force is set different from zero [2], see Figure 3. In contrast to this, "bias currents" are required in classical linear approaches. These lead to large Joule effect losses, which can be avoided with the flatness-based nonlinear control.

In two measurement planes (perpendicular to the x-direction) at $x = l_{m,v}$ and $x = -l_{m,h}$ the deviation $Y_{m,v}$, $Y_{m,h}$, $Z_{m,v}$, and $Z_{m,h}$ from center position is measured in y- and z-direction:

$$\begin{aligned} Y_{m,v} &= Y + l_{m,v}\theta, \qquad & Y_{m,h} &= Y - l_{m,h}\theta \\ Z_{m,v} &= Z - l_{m,v}\psi, \qquad & Z_{m,h} &= Z + l_{m,h}\psi. \end{aligned} \tag{4}$$

In the sequel we will refer to the plane at $x = l_{m,v}$ as the v-measurement plane. These equations can be solved for the generalized coordinates Y, Z, θ, and ψ. A fifth sensor measures the axial position X. Finally, the angular position ϕ is measured by means of an incremental encoder.

The above equations reflect the dynamics of the unperturbed system. Modelling errors (for example due to an incorrect relation between the input currents $i_\bullet$ and the corresponding force $F_\bullet$) have the same effect as constant disturbance forces when the task of stabilization at a constant position is considered. These forces are estimated by the observer presented later.

The rotation of the shaft is a source of disturbances with a significant harmonic component:

- The induction motor not only generates the torque driving the rotation about the x-axis but also creates forces in radial direction.
- When the shaft moves on an elliptic trajectory, the position in y- and z-direction is a sinusoidal function of time. A significant part of error in the relation between current and force can be expected to change sinusoidally, too, since the relation depends on the air-gap length (i. e., the position of the shaft).
- When the tool is cutting with varying depth the resulting forces are expected to change sinusoidally.

All these harmonic disturbance forces have in common, that their frequency is close to the rotational speed ω and that their amplitude and direction is unknown. Therefore, the effective harmonic disturbance force needs to be estimated for compensation purposes (see section "observer design").

FLATNESS-BASED TRAJECTORY TRACKING CONTROLLER

Considering the equations of motion (1) auxiliary (acceleration) variables can be introduced as $a_x, a_y, a_z, \alpha_\psi, \alpha_\theta, \alpha_\phi$:

$$\begin{aligned}
m\,a_x &= F_x + m\,g_x \\
m\,a_y &= F_{v,y} + F_{h,y} + m\,g_y \\
m\,a_z &= F_{v,z} + F_{h,z} + m\,g_z \\
\Theta_2\,\alpha_\psi &= -(l_{f,v} - X)F_{v,z} + (l_{f,h} + X)F_{h,z} - \Theta_1\,\dot\phi\,\dot\theta \\
\Theta_2\,\alpha_\theta &= (l_{f,v} - X)F_{v,y} - (l_{f,h} + X)F_{h,y} + \Theta_1\,\dot\phi\,\dot\psi \\
\Theta_1\,\alpha_\phi &= D_\phi .
\end{aligned} \tag{5}$$

With these we obtain the six decoupled subsystems

$$\ddot X = a_x, \quad \ddot Y = a_y, \quad \ddot Z = a_z,$$
$$\ddot\psi = \alpha_\psi, \quad \ddot\theta = \alpha_\theta, \quad \ddot\phi = \alpha_\phi,$$

for which linear controllers stabilizing the tracking error dynamics can be designed. For example, for the position X one uses

$$a_x = \ddot X_{\mathrm{ref}} - k_1\dot e_x - k_0 e_x, \tag{6}$$

where X_{ref} is a twice differentiable reference trajectory and the controller gains are $k_0, k_1 > 0$. The tracking error $e_x := X - X_{\mathrm{ref}}$ now satisfies

$$\ddot e_x + k_1\dot e_x + k_0 e_x = 0. \tag{7}$$

Using (6), we compute the auxiliary accelerations $a_x, \ldots, \alpha_\phi$. From these accelerations the forces and the torque D_ϕ are obtained by solving the inhomogeneous linear system (5). Finally, for a positive force $F_\bullet$ the control current $i_{\bullet,p}$ in the corresponding winding is obtained from

$$i_{\bullet,p} = \sqrt{\frac{F_\bullet}{k_{\bullet,p}}}(\sigma_{\bullet,p} - s_{\bullet,p}), \tag{8}$$

while the current $i_{\bullet,n}$ (generating a negative force) is kept zero. (For negative force $F_\bullet$ the currents $i_{\bullet,p} = 0$ and $i_{\bullet,n} = \sqrt{-F_\bullet/k_{\bullet,n}}(\sigma_{\bullet,n} - s_{\bullet,n})$ are used.) This approach avoids bias currents required in classical linear approaches: at any instant there is a current in only one coil of each pair [2], see Figure 3. The above design is based on the *differential flatness* of the model: The coordinates $X, Y, Z, \phi, \theta, \psi$ form a flat output of the mechanical subsystem [1] — see the appendix for the notion of differential flatness.

The trajectory planning is simplified by the flatness property. For example, if we want to transfer the center of mass of the shaft within time t^* from the center position onto an elliptic trajectory we choose

$$\begin{aligned}
Y_{\mathrm{ref}}(t) &= r_y(t)\,\cos\Omega t \\
Z_{\mathrm{ref}}(t) &= r_z(t)\,\sin\Omega t \\
X_{\mathrm{ref}}(t) &= \psi_{\mathrm{ref}}(t) = \theta_{\mathrm{ref}}(t) = 0 \\
\phi_{\mathrm{ref}} &= \omega_0\,t + \phi_0 \qquad (\omega_{\mathrm{ref}} = \omega_0 = \text{const.})
\end{aligned} \tag{9}$$

for the components of the flat output $(X, Y, Z, \phi, \psi, \theta)$ and

$$r_y(t) = r_y^*\,p(t), \qquad r_z(t) = r_z^*\,p(t)$$

with

$$p(t) = 10\left(\frac{t}{t^*}\right)^3 - 15\left(\frac{t}{t^*}\right)^4 + 6\left(\frac{t}{t^*}\right)^5 .$$

OBSERVER DESIGN

We only treat the design of an observer for the Z-coordinate of the center of mass. Using the measurements $Z_{m,v}$ and $Z_{m,h}$ we can calculate Z according to (4) and thus Z is assumed to be measured. The observer estimates the velocity $Z_v = \dot{Z}$ and a disturbance acceleration d_z, caused by modelling errors.

The differential equation describing the motion in z-direction is

$$\ddot{Z} = a_z + d_z, \tag{10}$$

where a_z is the acceleration of the center of mass due to bearing forces $F_{v,z}$, $F_{h,z}$ and gravity (see (5)). The quantity $d_z = d_{zc} + d_{zh}$ is an unknown disturbance acceleration which is assumed to be the sum of a constant and a sinusoidal function of time with a known constant frequency ω_d. Thus, the observer can be written as a simulator of the system extended by a stabilizing injection of the observation error $\tilde{Z} = Z - \hat{Z}$:

$$\begin{aligned}
\dot{\hat{Z}} &= \hat{Z}_v && + l_1\,\tilde{Z} \\
\dot{\hat{Z}}_v &= a_z + \hat{d}_{zc} + \hat{d}_{zh} && + l_2\,\tilde{Z} \\
\dot{\hat{d}}_{zc} &= && \, l_3\,\tilde{Z} \\
\dot{\hat{d}}_{zh} &= \hat{z}_5 && + l_4\,\tilde{Z} \\
\dot{\hat{z}}_5 &= -\omega_d^2 \hat{d}_{zh} && + l_5\,\tilde{Z}.
\end{aligned} \tag{11}$$

With the third equation of (11) we estimate the constant part ($\dot{d}_{zc} = 0$) and with the fourth and fifth equation the harmonic part of the disturbance d_z, i. e., $\ddot{d}_{zh} + \omega_d^2 d_{zh} = 0$. The observer gains $l_1, \ldots, l_5$ can be chosen such that the dynamics of the observer error $\tilde{Z}$ is stable.

EXPERIMENTAL RESULTS

The controller has been implemented on a dSPACE DS1103 controller board. The AXOMAT test bed has then been used to test the proposed algorithms.

In the first experiment, the shaft is rotating with an angular velocity of about 4800 rpm, i. e., $\omega = 500\mathrm{s}^{-1}$ and no material is cut off. The reference trajectory for the z-direction is of the type $Z_{\mathrm{ref}}(t) = r_z \cos\omega t$ with $r_z = 75\mu\mathrm{m}$. In Figure 3 the reference trajectory and the position measured in the v-measurement plane are shown. Note that the figure is only a “snapshot” and $t = 0$ in the figure does not correspond to the point $t = 0$ in the reference trajectory. Note also that there is no “phase shift” between the reference and the measured position, i. e., synchronism between the measured position and the reference trajectory has been achieved.

In the bottom plot of Figure 3 the currents in a horizontal bearing are shown. The mapping from bearing force to positive- and negative-direction currents is done by means of the so-called *almost current complementary function* (see [2]) rather than using (8). This essentially means the following: for larger forces only the coil current corresponding to the direction of the force is nonzero while the other current is zero, for smaller forces both coil currents are nonzero. This almost current complementary function is used in order to avoid a singularity (at $F_\bullet = 0$) related to the fact that the square-root function in (8) is not differentiable for $F_\bullet = 0$. This would require the current controllers to generate infinite voltages in order to track current references corresponding to a zero-crossing of the bearing force.

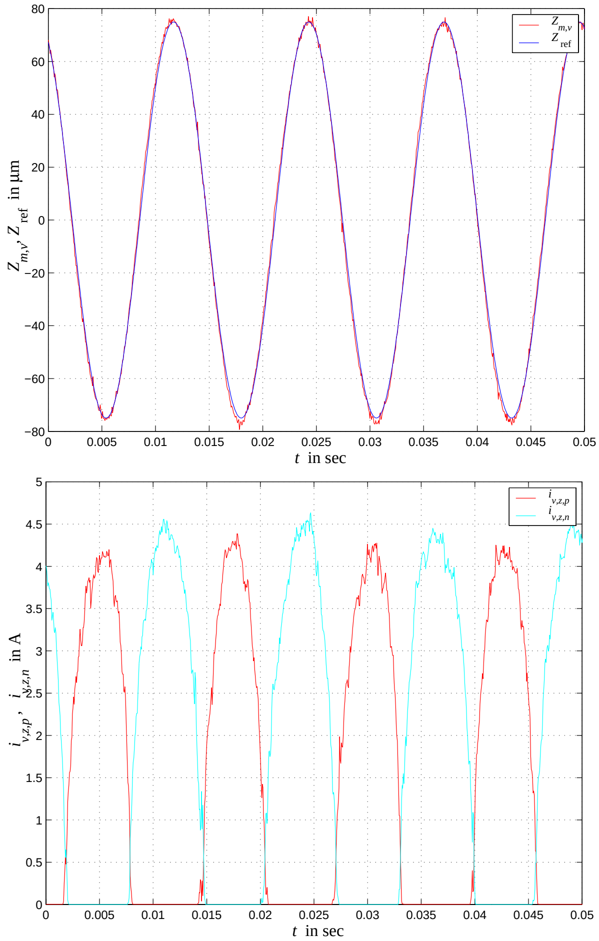

FIGURE 3: Trajectory tracking performance: while turning at about 4800rpm the horizontal position ($Z_{m,v}$, i. e., measured in the v-measurement plane) is tracking a sinusoidal reference Z_{ref} with an amplitude of $75\mu\mathrm{m}$, synchronized with the rotation about the x-axis. Bottom plot: currents in the z-direction coils in the v-bearing

Figure 4 shows the result of a drilling experiment in aluminium. The figure depicts the deviation of the shape of the drilled hole from a circular shape. It is important to note that the figure is not drawn to scale. The reason for this is to magnify the outer $30\mu\mathrm{m}$ region where the elliptic shape is carved. That is, the diameter of the inner solid circle is about $30\mathrm{mm}$ and the difference between major and minor axis length of the resulting ellipse is approximately $46\mu\mathrm{m}$ ($50\mu\mathrm{m}$ was desired). Using a dashed line we have drawn an ellipse (with the major axis length approximately $50\mu\mathrm{m}$ larger than the minor one into the diagram). With this, the deviation of the shape of the

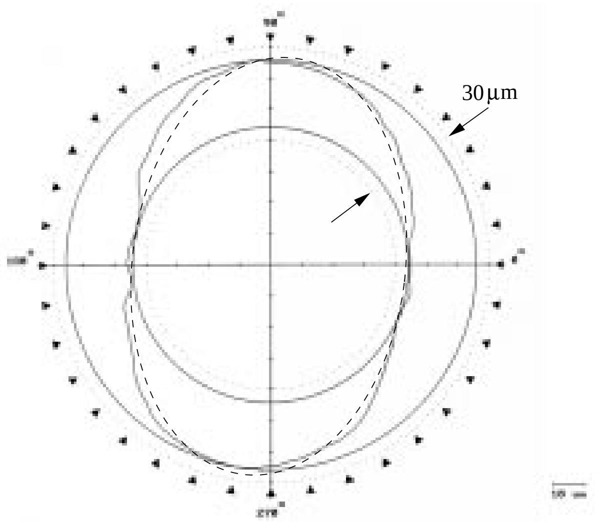

FIGURE 4: Deviation of the shape of a drilled elliptic hole from circular shape

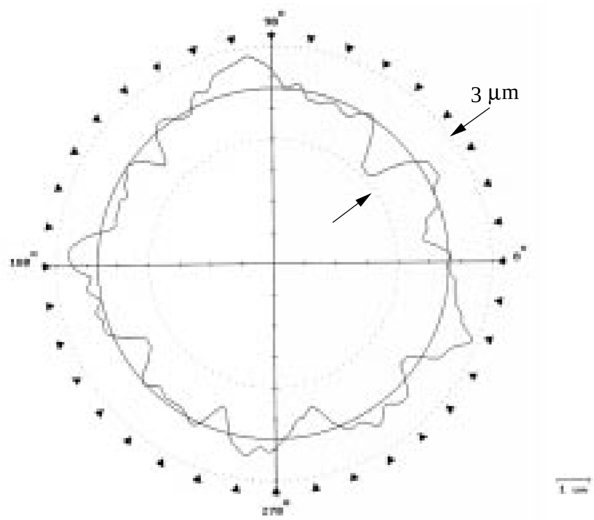

FIGURE 5: Deviation of the shape of a drilled circular hole from circular shape

hole from the desired elliptic shape can be judged. One reason for the axes of the ellipse not being oriented in the same direction as the axes of the diagram is that no special care has been taken in order to adjust the directions of the spindle with respect to the workpiece.

Figure 5 shows the result of an experiment where a circular hole was drilled. The deviation from circular shape is less than $2\mu\mathrm{m}$.

The measurements shown in Figure 6 were taken while drilling a hole with an elliptic shape at about 4800rpm. The plot at the top shows the measured and reference position in the v-measurement plane. The reference trajectories $Z_{\mathrm{ref}}(t), Y_{\mathrm{ref}}(t)$ for the center of mass of the shaft and the measured positions $Z_{m,v}(t), Y_{m,v}(t)$ are depicted in the bottom plot. Observe the excellent tracking of the reference trajectories. The trajectory parameters $(r_z, r_y) = (25\mu\mathrm{m}, 50\mu\mathrm{m})$ are chosen for an elliptic hole with the major axis length $50\mu\mathrm{m}$ larger than the minor axis length.

CONCLUSIONS AND FURTHER WORK

It has been shown that the proposed flatness-based path tracking control for a magnetically levitated spindle makes it possible to drill non-circular holes with high precision. Currently, drilling at higher angular velocities is investigated. Another control objective, interesting especially at high rotation speeds, is the inertial autocentering of the spindle which reduces the bearing forces due to inertial imbalance of the shaft.

ACKNOWLEDGMENTS

This work is part of a research project financially supported by the European Union (EFRE) and the Free State of Saxony (P-No. 5051).

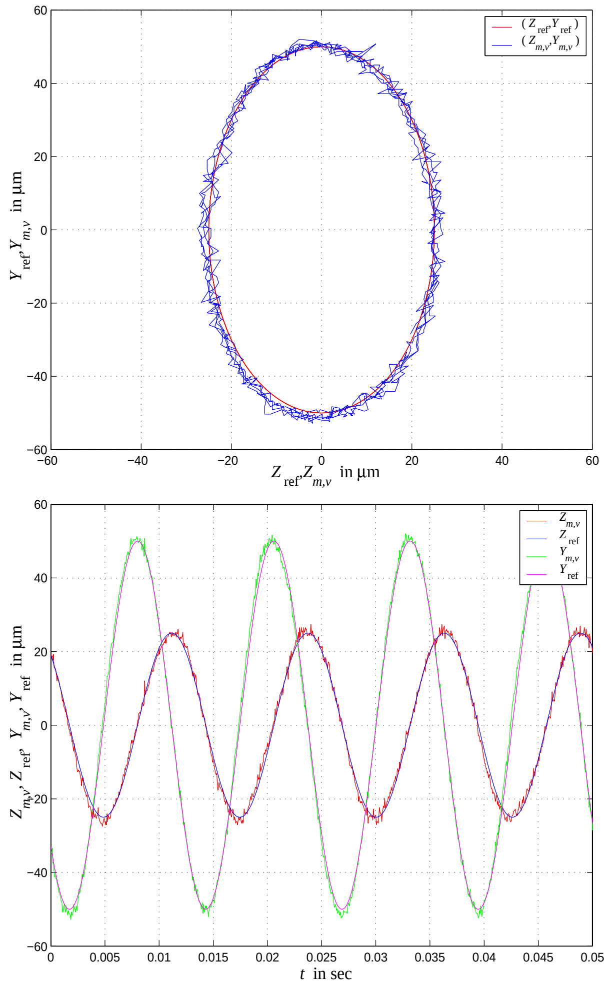

FIGURE 6: Top: position in the v-measurement plane while drilling a hole with elliptic shape at 4800 rpm. Bottom: corresponding reference trajectories and measured position in vertical and horizontal direction

APPENDIX

The notion of flatness has been introduced by M. Fliess, J. Lévine, Ph. Martin, and P. Rouchon several years ago, and there are now quite a few introductory references available: e. g., [1, 3, 5].

We consider systems defined by a *generalized state representation* with input $u = (u_1, \ldots, u_m)$ and *(generalized) state* $x = (x_1, \ldots, x_n)$, i. e., by a set of first order ordinary differential equations

$$\dot{x}_i = F_i(x, u, \ldots, u^{(\alpha_i)}), \quad i = 1, \ldots, n. \tag{12}$$

Such a system is called *(differentially) flat* if there exists a set $(y_1, \ldots, y_m)$ of functions

$$y_i = h_i(x, \dot{u}, \ldots, u^{(\beta_i)}), \quad i = 1, \ldots, m, \tag{13}$$

called a *flat (or linearizing) output*, with the following two properties:

1. The components of y are not related by any differential equation of the form:

$$P(y, \dot{y}, \ldots, y^{(\gamma)}) = 0$$

2. All the components of the state x and of the input u can be calculated from y and its derivatives. In other words, these variables can be expressed, respectively, as

$$x_i = A_i(y, \dot{y}, \ldots, y^{(\gamma_i)}), \quad i = 1, \ldots, n$$

and

$$u_i = B_i(y, \dot{y}, \ldots, y^{(\delta_i)}), \quad i = 1, \ldots, m.$$

As a consequence of the second property, also the derivatives of x and u, and all functions of those variables can be expressed as functions of y and its derivatives. The trajectories for y can be chosen freely as a consequence of the first property. Actually, by a choice of y with m components, i. e., with as much components as the input u, the second property implies the first one.

REFERENCES

[1] M. Fliess, J. Lévine, P. Martin, and P. Rouchon. Flatness and defect of non-linear systems: introductory theory and examples. *Int. J. Control*, 61(6):1327–1361, 1995.

[2] J. Lévine, J. Lottin, and J.-Ch. Ponsart. A nonlinear approach to the control of magnetic bearings. *IEEE Trans. on Control Systems Technology*, 4(5):524–544, 1996.

[3] Ph. Martin, R.M. Murray, and P. Rouchon. Flat systems. In *Plenary Lectures and Mini-Courses, European Control Conference*, pages 211–264, Brussels, Belgium, July 1997.

[4] J.-Ch. Ponsart. *Asservissements numériques de paliers magnétiques. Application aux pompes à vide*. Thèse de Doctorat, Université de Savoie, Annecy, France, 1996.

[5] R. Rothfuß, J. Rudolph, and M. Zeitz. Flachheit: Ein neuer Zugang zur Steuerung und Regelung nichtlinearer Systeme. *at — Automatisierungstechnik*, 45(11):517–525, 1997.

[6] J. Rudolph, F. Woittennek, and J. von Löwis. Zur Regelung einer elektromagnetisch gelagerten Spindel. *at — Automatisierungstechnik*, 48(3):132–139, 2000.

[7] G. Schweitzer, A. Traxler, and H. Bleuler. *Magnetlager*. Springer Verlag, Berlin, Heidelberg, 1993.

[8] J. Thiele and F. Urban. Motorspindeln mit aktiven Magnetlagern erhöhen Leistungsfähigkeit von Maschinen. *Maschinenmarkt*, 52:30–33, 1998.